Proc. International Conference on Mechanical, Automotive and Mechatronics Engineering (ICMAME 2023)
29-30 April 2023, Dubai, UAE

Study on the Influence of Engine Stack Length on the Efficiency of A Heat-driven Thermoacoustic Refrigerator

Irna Farikhah
Department of Mechanical Engineering
Universitas PGRI Semarang
Semarang, Indonesia
irnafarikhah@upgris.ac.id

Akbar Muslim
Department of Mechanical Engineering
Universitas PGRI Semarang
Semarang, Indonesia
akbar@gmail.com

Aan Burhanuddin
Department of Mechanical Engineering
Universitas PGRI Semarang
Semarang, Indonesia
aanburhanudin@upgris.ac.id

Agus Mukhtar
Department of Mechanical Engineering
Universitas PGRI Semarang
Semarang, Indonesia
agusmukhtar@upgris.ac.id

Maroua Ben Nasr
Department of Physics
University of Tunis El Manar
Tunis, Tunisia
maroua@gmail.com

Ahmad Nadhif Masruri
Department of Mechanical Engineering
Universitas Diponegoro
Semarang, Indonesia
ahmadnadifmasrur@student.undip.ac.id

***Abstract*— The Scarcity of renewable energy is one of the world issues that must be tackled. Moreover, the necessity of environmentally friendliness cooler is indispensable nowadays. There is an alternative technology which can handle the issues. Using thermoacoustic engine the waste heat and solar energy can be converted into acoustic energy that can be used for thermoacoustic cooler which is safe for environment. The aim of the study is to obtain the influence of engine stack/regenerator length on the efficiency of a heat-driven thermoacoustic refrigerator. The investigation was conducted numerically to find the optimum value of the regenerator length. It was found that the regenerator length is 0.014. Furthermore, the engine and cooler efficiency are 52 % and 36 % of the Carnot efficiency. In addition, the lowest heating temperature of the engine is 241℃ which is good for exhaust heat recovery and green energy.**

Keywords— heat-driven, machine, refrigerator

I. INTRODUCTION

Nowadays the lack of renewable energy is becoming the urgent issues all over the world [1]. Therefore, it is essential to tackle the problem. It can be handled using thermoacoustic technology. We could convert waste heat, geothermal and solar energy into sound energy by using thermoacoustic machine [2]. The engine can be used for driving cooler or electric power generation [3-6]. In other words, the acoustic power can be converted into electrical power [7].

On the other hand, the environmental issues such as depletion ozone layer and global warming potential are also need to be handled [8]. Thermoacoustic cooler technology can be a solution for it. In thermoacoustic, there is a cooler driven by an electrodynamic loudspeaker done by Farikhah et.al. They found that there is a decrease of the cooling temperature of 5 ℃ [9]. However, the cooler relies on the non-renewable energy, so it is essential to use the renewable energy for example exhaust heat or sunlight energy. The device for converting the energy is called thermoacoustic engine. The energy conversion can be calculated using the thermoacoustic theory. Ueda in 2016 numerically calculated the energy conversion in the regenerator screen [10]. Some researchers also studied about the engine and analyzed the heating temperature and the performance. The numerical study was conducted by Utami et.al. They focused on the effect of the radius of the engine stack to the performance of thermoacoustic engine. Rokhmawati in 2020 investigated the mean pressure and pipe's radius impact on the efficiency of the entire device. Furthermore, Farikhah in 2021 numerically studied the influence of stack length on the performance of thermoacoustic engine. However, this is without the load such as a thermoacoustic cooler [11-13]. The engine can be combined with the cooler. In other words, thermoacoustic cooler can be driven by the thermoacoustic machine. In 2017 there is a study on the performance of a heat-driven thermoacoustic cooler with different porosity [4]. In 2017 Farikhah studied the efficiency of a thermoacoustic system with machine and refrigerator stack in a pipe [5]. The influence of mean pressure on the efficiency of a heat-driven thermoacoustic chiller was studied in 2020 [6]. However, the heating temperature of the machine is still high [4-6]. Therefore, it is important to find the low heating temperature for waste heat recovery which is beneficial for renewable energy. To obtain the low heating temperature of the machine, the multistage engine must be set up. There is an investigation the influence of stack radii on the efficiency of multistage machine [14]. However, in this case we need to installed 4 regenerators which is more complicated. Therefore, designing the simple and efficient device with low heating temperature such as single stage cooler driven by engine is essential due to the simplicity. In this case, the dimensionless engine regenerator length L_s/L_{loop} is the parameter. Thus, in this investigation we focus on finding the impact of engine stack length on the performance of the cooler driven by the machine. We focus on the efficiency of the whole system because it

means that we focus on decreasing the dissipation. Thus, in the future it will be good for commercial cooler industry.

II. METHOD

A. Calculation Model

The Design of a heat driven thermoacoustic cooler is presented in Fig. 1. It comprises of two stacks, four heat exchangers and two thermal buffer tubes which is filled with helium and the pressure is 3 MPa. The looped tube length is 280 cm and the diameter is 4 cm. The first regenerator is employed as an engine and the second regenerator is employed as a cooler. The engine is located between the ambient and hot heat exchanger. In the vicinity of the heat exchanger is set a thermal buffer tube to allow the temperature change gradually from heating temperature T_h to to ambient temperature T_a. The cooler is placed between the ambient and cold heat exchanger. Another thermal buffer tube is put next to the cold heat exchanger allowing the cooling temperature increasing gradually T_c to the ambient temperature T_a. T_c and T_a are set at 0℃ and 28 ℃, respectively, whilst the heating temperature is obtained as a result of stability limit calculation [15]. The length of the engine regenerator is varied between 30 mm to 90 mm which are set as the parameter, while the cooler length is set as a constant value at 40 mm. In addition, the narrow channel radius of the machine and refrigerator stack are 0.1 mm and 0.5 mm, respectively.

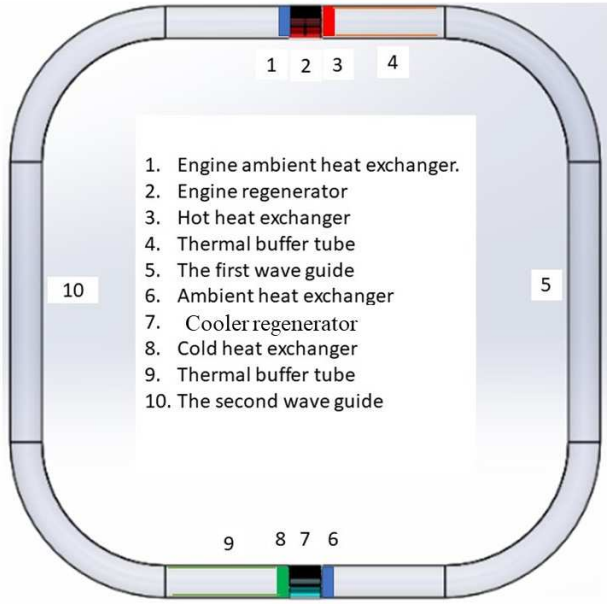

Fig. 1. Design of a heat-driven thermoacoustic refrigerator

TABLE I. model of the cooler driven by the engine

The geometrical Parameter	Value
Engine ambient heat exchanger length Engine ambient heat exchanger radius Engine ambient heat exchanger porosity	10 mm 0.5 mm 0.5
Engine Regenerator/stack length Engine Regenerator/stack porosity Engine regenerator/stack flow channel radius	30-90 mm 0.77 0.1 mm
hot heat exchanger length hot heat exchanger radius hot heat exchanger porosity	10 mm 0.5 mm 0.5
engine Thermal buffer tube length engine Thermal buffer tube diameter	600 mm 40 mm
The first wave guide length The first wave guide diameter	740 mm 40 mm
Cooler ambient heat exchanger length Cooler ambient heat exchanger diameter	10 mm 40 mm
Cooler Regenerator/stack length Cooler Regenerator/stack flow channel radius Cooler regenerator/stack porosity	40 mm 0.5 mm 0.77
Cold exchanger length Cold exchanger diameter	10 mm 40 mm
Cooler Thermal buffer tube length Cooler Thermal buffer tube diameter	600mm 40mm
The second wave guide length The second wave guide diameter	740mm 40 mm

B. Calculation Method

In the simulation, we use these two equations who is derived by Rott shown in eq. 1 and eq. 2. [16]. The axial coordinate along the pipe is expressed as x where the initial point is set at the engine regenerator ambient side. $\delta, \chi_v,$ and χ_α are the thermal penetration depth and the thermoacoustic function. The mean density, specific heat ratio and the Prandtl number of Helium are denoted as $\rho_{m,}\gamma$ and σ, respectively. The pressure and velocity are denoted as P and U, respectively.

If $dT_m/dx = 0$, eq. (1) and eq. (2) can be solved analytically, but if $dT_m/dx \neq 0$, the two equations have to be computationally integrated [15]. We used two temperature conditions. The constant value of dT_x/dm is the first condition and the calculated value of dT_x/dm is the second conditions. Here, the constant enthalpy flow along the regenerator is set. It is denoted as $\dot{H}$ [see eq. 3]

$$\frac{dP_1}{dx} = -\frac{i\omega\rho_m}{1-\chi_v}U_1 \tag{1}$$

$$\frac{dU_1}{dx} = -\frac{i\omega[1+(\gamma-1)\chi_\alpha]}{\gamma P_m}P_1 + \frac{\chi_\alpha-\chi_v}{(1-\chi_v)(1-\sigma)}\frac{1}{T_m}\frac{dT_m}{dx}U_1 \tag{2}$$

$$\dot{H} = \dot{W} - \dot{Q} \tag{3}$$

As eq. 1 and 2 is substituted into eq. 3, so the equation become as follow

$$dT_m/dm = \frac{\dot{H} - \frac{A}{2}Re\left[P\tilde{U}\left(1 - \frac{\tilde{\chi}_v - \chi_\alpha}{(1+\sigma)(1-\tilde{\chi}_v)}\right)\right]}{\frac{A\rho_m c_p |U|^2}{2\omega(1-\sigma^2)|1-\chi_v|^2} Im[\chi_\alpha + \sigma\tilde{\chi}_v]} \quad (4)$$

Using eqs. 1-4, temperature gradient along the regenerators can be calculated if the boundary conditions of the oscillatory pressure P and Velocity U are given. In this calculation, the thermal conduction and the acoustic streaming are neglected [17,18,19]. In this simulation the heating temperature T_h , angular frequency ω and impedance P/U are calculated using the stability limit calculation [15].

Equation 1 and 2 are converted in a matrix form.

$$\frac{d}{dx}\begin{pmatrix} P_1(x,t) \\ U_1(x,t) \end{pmatrix} = C(x)\begin{pmatrix} P_1(x,t) \\ U_1(x,t) \end{pmatrix} \quad (5)$$

$$C(x) \equiv \begin{pmatrix} 0 & \frac{-i\omega\rho_m}{1-\chi_v} \\ \frac{-i\omega[1+(\gamma-1)\chi_\alpha]}{\gamma P_m} & \frac{\chi_\alpha - \chi_v}{(1-\chi_v)(1-\gamma)}\frac{1}{T_m}\frac{dT_m}{dm} \end{pmatrix} \quad (6)$$

$$\begin{pmatrix} P_1(x+\Delta x,t) \\ U_1(x+\Delta x,t) \end{pmatrix} = \left(E + \Delta x C'(x)\right)\begin{pmatrix} P_1(x) \\ U_1(x) \end{pmatrix} \quad (7)$$

$$C'(x) = \frac{1}{6}(RK_1 + 2RK_2 + 2RK_3 + RK_4) \quad (8)$$

Here, we used the Fourth-order Rung Kutta Method

$$RK_1 = C(x) \quad (9)$$

$$RK_2 = C\left(x + \frac{\Delta x}{2}\right)\left(E + \frac{\Delta x}{2}RK_1\right)$$

$$RK_3 = C\left(x + \frac{\Delta x}{2}\right)\left(E + \frac{\Delta x}{2}RK_2\right)$$

$$RK_4 = C(x + \Delta x)(E + \Delta x RK_3)$$

The unit matrix is denoted as E

$$\begin{pmatrix} P_1(x,t) \\ U_1(x,t) \end{pmatrix} = M_{II}(x,x_0)\begin{pmatrix} P_0(x_{0,},t) \\ U_0(x_0,t) \end{pmatrix} \quad (10)$$

$$M_{II}(x,x_0) \equiv (E + \Delta x C'_{n-1})(E + \Delta x C'_{n-2}) \dots (E + \Delta x C'_1)(E + \Delta x C'_0) \quad (11)$$

The partition number between x_o and x is expressed as *n*.

$$Y_{d,e} = \begin{pmatrix} 1 & 0 \\ 0 & A_d/A_e \end{pmatrix} \quad (12)$$

There are 10 components in a heat-driven thermoacoustic refrigerator as mentioned in table. 1.

Here, the subscript *d* and *e* denote the component's number. The total path area is denoted as *A*. the total system transfer matrix is expressed as:

$$M_{tot} = M_{10}O_{10,9}M_9O_{9,8}M_8O_{8,7}M_7O_{7,6}M_6O_{6,5}M_5O_{5,4}M_4O_{4,3}M_3O_{3,2}M_2O_{2,1}M_1 \quad (13)$$

$$M_{tot}\begin{pmatrix} P_{e,A} \\ U_{e,A} \end{pmatrix} = \begin{pmatrix} P_{e,A} \\ U_{e,A} \end{pmatrix} \quad (14)$$

If the determinant of the matrix $(M_{tot} - E)$ is zero, the solution $P_{e,a,}U_{e,a}$ of equation 15 is nonzero

$$(m_{11} - 1)(m_{22} - 1) - m_{12}m_{21s} = 0 \quad (15)$$

The element of M_{tot} is denoted as m_{ij}, so equation 15 was solved to obtain the stability limit conditions that shows the gas spontaneously oscillates.

The total efficiency of the whole thermoacoustic refrigerator system can be expressed as:

$$\eta_{all} = \eta_{2,e}.\eta_{2,c}.\eta_{tube} \quad (16)$$

Where $\eta_{all,2}$ is the entire efficiency in the whole system. $\eta_{all,2}$ is divided into three efficiencies; $\eta_{2,e}$ is the second law efficiency of the engine, $\eta_{2,c}$ is the second law of the cooler and η_{tube} is the efficiency of the pipe.

$$\eta_{2,e} = \eta_e/\eta_{Carnot} \quad (17)$$

$\eta_{2,e}$ is defined as eq. 17, thermal and Carnot efficiency are denoted as η_e and η_{Carnot}.

$$\eta_e = \Delta\dot{W}_e/\dot{Q}_h \quad (18)$$

where $\Delta\dot{W}_e$ is the acoustic power gain and $\dot{Q}_h$ is the heating power.

$$\eta_{Carnot} = (T_h - T_a)/T_h \quad (19)$$

$$\eta_{2,c} = COP/COP_{Carnot} \quad (20)$$

COP is Coefficient of Performance of the refrigerator and COP_{Carnot} is Carnot COP.

$$COP = \dot{Q}_c/\Delta\dot{W}_c \quad (21)$$

The refrigeration and the acoustic power consumed by the cooler are defined as $\dot{Q}_c$ and $\Delta\dot{W}_c$, respectively.

$$COP_{Carnot} = T_C/(T_a - T_c) \quad (22)$$

$$\eta_{tube} = \Delta\dot{W}_c/\Delta\dot{W}_e \quad (23)$$

η_{tube} is the ratio of acoustic power absorbed by refrigerator to the acoustic power generated by the machine.

III. RESULTS AND DISCUSSIONS

A. Performance of the whole System

Figure 2 shows the validation between the numerical calculation and the experimental one. As we can see, the pressure amplitude $|P|$, Velocity $|U|$ and the phase different φ have a good agreement between the calculation and the experimental work.

The entire performance of the cooler system $\eta_{2,all}$ is provided in Fig. 3. The performance comprises of efficiency of machine, tube and cooler. In this simulation, the regenerator length L_s is varied from 3 cm to 9 cm and the loop tube length L_{loop} is 280 cm. In this calculation, we used the dimensionless

ratio of the stack and the pipe lengths as the parameter denoted as L_s/L_{loop}. As we can see in fig. 3, when L_s/L_{loop} rise from 0.010 to 0.014 η_{all} increase from 3.0 % to 4.0 % of Carnot efficiency. Then, when L_s/L_{loop} increase from 0.014 to 0.30 η_{all} drop from 4 % to 3 % of Carnot efficiency. According to eq.16, the whole efficiency of the system depends on the scond law efficiency of the engine $\eta_{2,e}$, cooler $\eta_{2,c}$ and tube η_{tube}, so it is essential to reveal those efficiency.

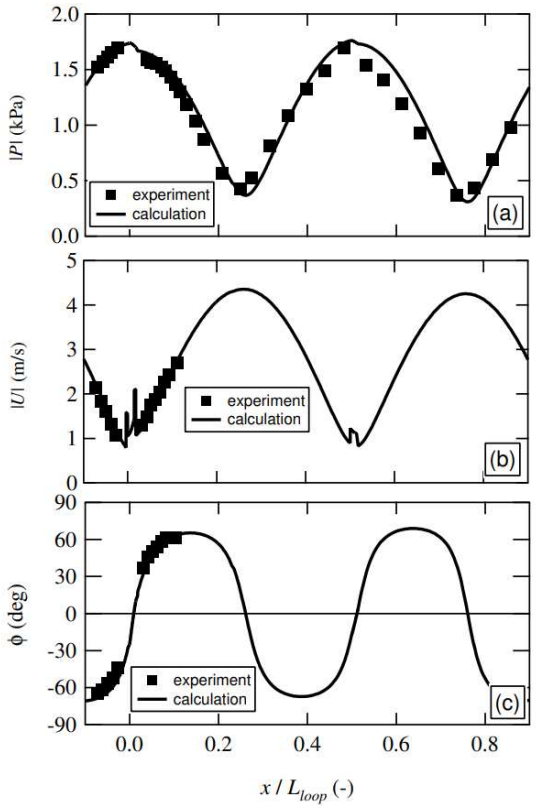

Fig. 2. |P|, |U|, and φ as a function of x/L_{loop}. The symbols show the experimental results obtained from the article [5, 20].

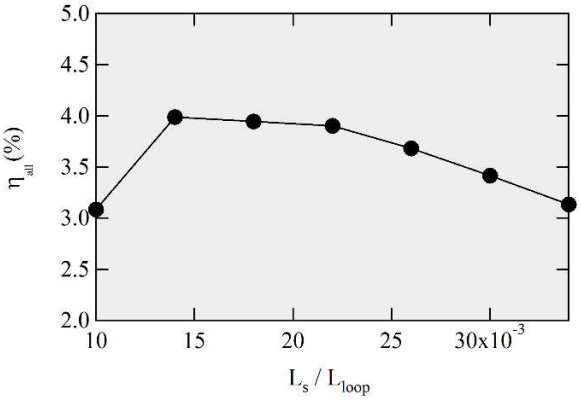

Fig. 3. η_{all} vs L_s/L_{loop}

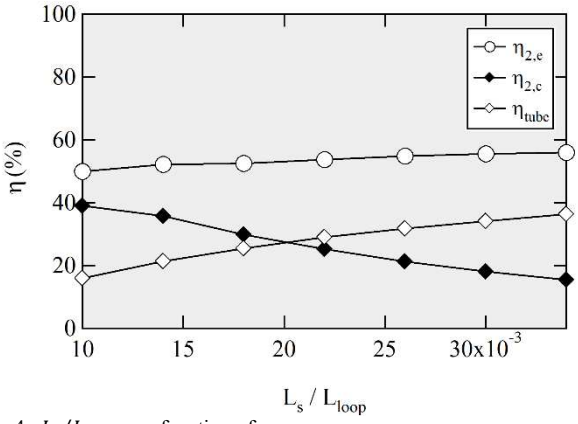

Fig. 4. L_s/L_{loop} as a function of $\eta_{2,e}$, $\eta_{2,c}$, η_{tube}

As mentioned above, the superior total performance of the device is achieved when the length is 0.014. According to figure 4, the superior efficiency of the device is due to the high value of all components. The efficiency of the engine, cooler and tube are 52 %, 32 % and 21 % of the upper limit value.

As we can see in Figure 4, $\eta_{2,e}$ has the highest value compare to the $\eta_{2,c}$ and η_{tube}. Furthermore, as L_s/L_{loop} go up from 0.010 to 0.030, $\eta_{2,e}$ rise from 50 % to 56 % of the upper limit values. On the other hand, η_{2c} drop from 39 % to 15 % when L_s/L_{loop} increase, while η_{tube} increase from 16 to 36 % when L_s/L_{loop} rise from 0.010 to 0.030.

Based on eq. 20, the second law efficiency of the refrigerator depends on COP and COP_{Carnot}. As we can see in the fig. 5, the high value of second law efficiency of the refrigerator is because of the high value of COP. When L_s/L_{loop} is 0.014, COP is 3.5. the highest value is when the length is 0.010 at 3.8, but the superior entire cooler system is at 0.014. It is because the engine and tube efficiency at 0.014 are higher than that of at 0.010 [see figure 4]. Therefore, in this study, we focus on the value of COP especially at 0.014. Moreover, the COP_{Carnot} are set at 9.75 since the cooling and ambient temperature are set at 0 ℃ and 28 ℃.

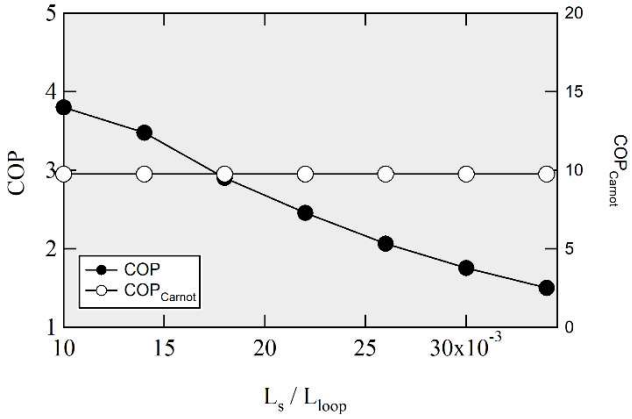

Fig. 5. L_s/L_{loop} VS of COP and COP_{Carnot}

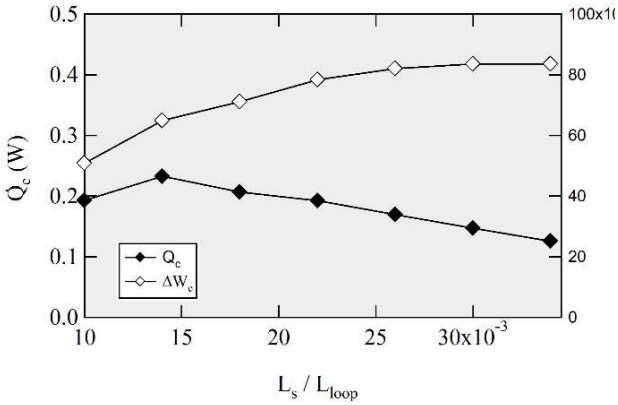

Fig. 6. L_s/L_{loop} VS of Q_c and Q_h

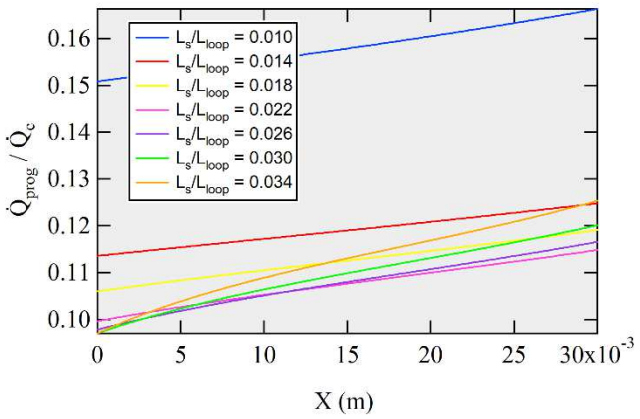

Fig. 7. L_s/L_{loop} as a function of $\dot{Q}_{prog}/\dot{Q}_c$

COP is the ratio of the cooling power $\dot{Q}_c$ to the acoustic power consumed by the cooler $\Delta\dot{W}_c$ as we can see in eq. 21. Therefore, the high value of *COP* can be attributed to the high value of cooling power $\dot{Q}_c$ as shown in Fig. 6. It shows the highest cooling power when the length is 0.014. It was found that the highest cooling power is 0.23 W. The cooling power is the summation between three different power that can be expressed as follows [21].

$$\dot{Q}_c = \dot{Q}_{prog} + \dot{Q}_{stand} + \dot{Q}_d \qquad (24)$$

Figure 7 shows the dimensionless parameter of $\dot{Q}_{prog}$, $\dot{Q}_{stand}$ and $\dot{Q}_d$ to $\dot{Q}_c$. $\dot{Q}_{prog}/\dot{Q}_c$ implies the travelling wave [20]. Figure 8 shows $\dot{Q}_{stand}/\dot{Q}_c$ implies the standing wave and figure 9 shows $\dot{Q}_d/\dot{Q}_c$ implies the dream pipe [21]. Compare to $\dot{Q}_{stand}$ and $\dot{Q}_d$, $\dot{Q}_{Progg}$ is the power which has high contributions on the high performance due to the reversible energy conversion which means less dissipation. As can be seen in figure 7, the highest $\dot{Q}_{progg}/\dot{Q}_c$ is achieved when the length ratio L_s/L_{loop} is 0.010 followed by 0.014. In fig. 8 the highest $\dot{Q}_{stand}/\dot{Q}_c$ is reached when the length ratio is 0.010. As $\dot{Q}_{stand}$ implies the standing wave, so at this length the irreversible energy conversion occurs. Eventhough $\dot{Q}_{progg}/\dot{Q}_c$ is highest at 0.010, but $\dot{Q}_{stand}/\dot{Q}_c$ is high as well. It indicates that at 0.010, the dissipation occurs more than that at 0.014. As a result, the most efficient would achieved when the length is 0.014.

$\dot{Q}_{prog}/\dot{Q}_c$ and $\dot{Q}_{stand}/\dot{Q}_c$ shown in Fig. 8 and 9 have positive values. It indicates that the flow directions of the cooling energy are the same. However, $\dot{Q}_d/\dot{Q}_c$ has negative values. It means that the flow direction of the cooling energy is the opposite direction. As a consequence, when $\dot{Q}_d$ is high the total $\dot{Q}_c$ decrease. Since at 0.010 the value of $\dot{Q}_d/\dot{Q}_c$ is the highest one, so the total $\dot{Q}_c$ will decrease at L_s/L_{loop}=0.010. Thus, the most efficient is when the L_s/L_{loop} is 0.014 due to the high value of $\dot{Q}_{prog}$ while $\dot{Q}_{stand}$ and $\dot{Q}_d$ are lower than that at 0.010.

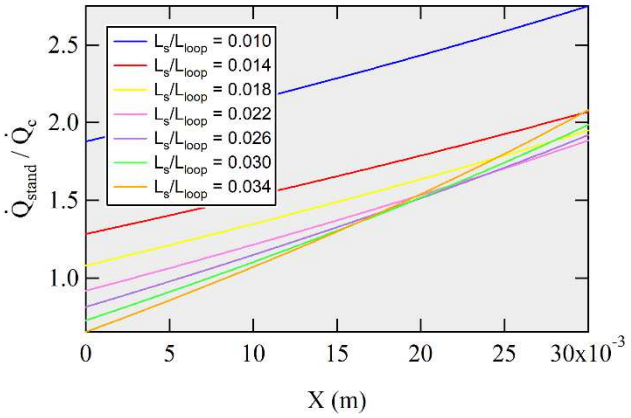

Fig. 8. L_s/L_{loop} as a function of $\dot{Q}_{stand}/\dot{Q}_c$

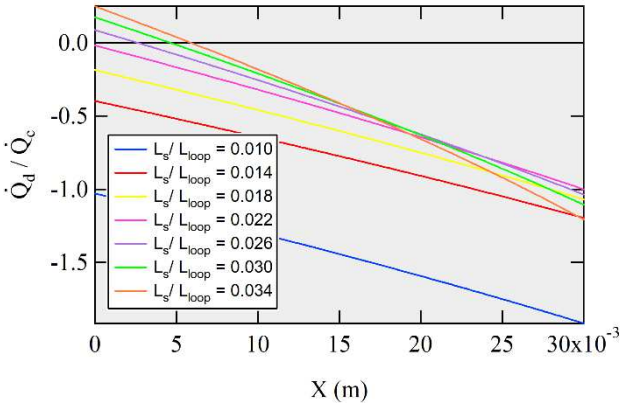

Fig. 9. L_s/L_{loop} as a function of $\dot{Q}_d/\dot{Q}_c$

B. The Heating Temperature

Figure 10 shows the engine regenerator length L_s/L_{loop} as a function of heating temperature T_h. The heating temperature increases from 241 ℃ to 386 ℃. At 0.010 the heating temperature is the lowest which can be used for waste heat recovery and renewable energy for generating the engine.

.

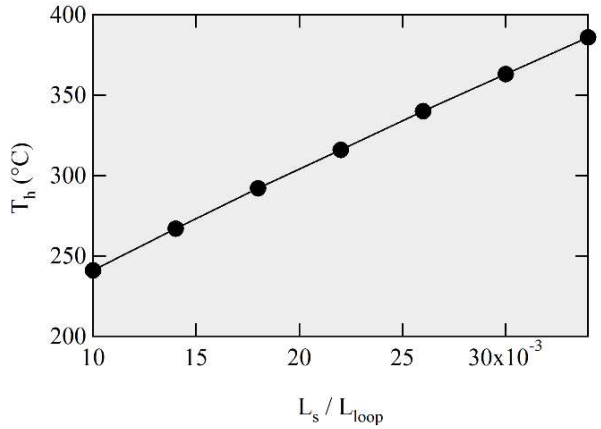

Fig. 10. L_s/L_{loop} as a function of T_h

IV. CONCLUSION

The influence of regenerator length on the efficiency of a heat-driven thermoacoustic refrigerator was investigated. It was found that when the dimensionless engine regenerator length is 0.014, the efficiency of the whole device is superior. The finding is essential for guidance in experimental work. It means when ratio of the stack length to the loop length is 0.014, the efficiency of the whole system is 4 % of the Carnot efficiency and the efficiency of the engine, cooler and tube are 52 % and 36 % and 21%, respectively. Moreover, the lowest heating temperature of the engine was found 241 ℃ at the length ratio 0.010. It means that the heating temperature can be used for exhaust heat recovery and green energy.

ACKNOWLEDGMENT

The investigation was supported by Indonesian government and Universitas PGRI Semarang. No. 002/LPPM-UPGRIS/SP2H/PENELITIAN/III/2022.

REFERENCES

[1] T. Yazaki; T. Biwa, A. Tominaga. A piston-less Stirling cooler. Appl. Phys. Lett. 2002, 80, 157–159.

[1] U. Shazat, ”The need for renewable energy sources”, International Journal of Information Technology and Electrical Engineering, 2012.

[2] D. L. Gardner, C. Q. Howard, ”Waste-heat-driven Thermoacaoustic Engine and Refrigerator”, Proceedings of ACOUSTICS 2009, Adelaide, Australia, 23-25 November 2009.

[3] A. Hamood, A. Jaworski, ”Experimental Investigation of the performance of a thermoacoustic electricity generator”, E3S Web of Conferences 116, 2019.

[4] I. Farikhah, Y. Ueda,” The effect of the porosity of regenerators on the performance of a heat-driven thermoacoustic cooler”, Proceeding of the 24th International Conference on Sound and Vibration (24 ICSV) London, 2017.

[5] I. Farikhah, Y. Ueda, ”Numerical calculation of the performance of a thermoacoustic system with engine and cooler regenerators in a looped tube”, Appl. Sci, vol. 7, pp. 672. 2017

[6] I. Farikhah, ”The effect of mean pressure on the performance of a single stage heat-driven thermoacoustic cooler. Int. J. Low-Carbon Technol. vol. 15, pp. 471–476, 2020.

[7] M. A. Hakim, M. Amiruddin, K. Hasto, Margono, I. Harjanto, Carsoni, I. Farikhah, Y. Setyoadi, H. Nuroso, U. Kaltsum, ”The Potential of Mechanic Vibration for Generating Electric Energy”, Advance Sustainable Science, Engineering and Technology (ASSET)”, vol. 2, 2020.

[8] S. Benhadid-Dib, A. Benzaoui, ”Refrigerants and their environmental impact Substitution of hydro chlorofluorocarbon HCFC and HFC hydro fluorocarbon. Search for an adequate refrigerant”, Energy Procedia, vol.18, pp. 807-816, 2012.

[9] I. Farikhah, S. Ristanto, H. Idrus, U. Kaltsum, A. Faisal, I. Setiawan, A. B. S. Utomo, ”Thermoacoustic design using stem of goose down regenerator”, American Institute of Physics (AIP) Conference Proceedings, vol. 1474, pp. 283-286, September 2012.

[10] Y. Ueda, I. Farikhah, ”Calculation of energy conversion efficiency of a regenerator-screen Regenerator using thermoacoustic theory, TEION KOGAKU (Journal of Cryogenics and Superconductivity Society of Japan), vol. 51, pp. 403-408, 2016.

[11] S. W. Utami, I Farikhah, N. Khoiri, S Patonah, U Kultsum, S. Suciati,”Numerical study of the influence of radius regenerator on the low heating temperature and efficiency of travelling wave thermoacoustic engine”, J. Phys.: Conf. Ser, vol. 1464, 2020.

[12] E.D. Rokhmawati, I. Farikhah, U. Kaltsum, H. Nuroso, A. Burhanudin, Y. Setyoadi, M. Amiruddin, I. A. Rahim, ”Numerical study on the effect of mean pressure and loop’s radius to the onset temperature and efficiency of travelling wave thermoacoustic engine”, Automotive Experiences, vol. 3, pp. 96-103, 2020.

[13] I. Farikhah, E. A. Elsharkawy, H. Nuroso, M. Novita, D. Marlina, ”Study of regenerator length on efficiency of thermoacoustic engine”, In Proceedings of the 3rd IEEE Eurasia conference on IOT, communication and engineering 2021, Yunlin, Taiwan, 2021.

[14] I. Farikhah, E. A. Elsharkawy, A. S. Saad, T. Atia, ”Numerical Study on the Effect of Regenerator Radii on the Low Onset Heating Temperature and Efficiency of 4-Stage Thermoacoustic Engine”. Arab J Sci Eng , 2022

[15] Y. Ueda, C. Kato,”Stability Analysis of Thermally Induced Spontaneous Gas Oscillations in Straight and Looped Tube”. Journal of Acoustical Society of America, 2008.

[16] N. Rott, Damped and thermally driven acoustic oscillations in wide and narrow tubes. Z. Angew. Math. Phys. 1969, 20, 230–243.

[17] G. W. Swift, Thermoacoustics A Unifying Perspective for Some Engines and Refrigerators; Acoustical Society of America, New York, USA, 2002.

[18] G.W. Swift, D. L. Gardner, S. Backhaus, “A thermoacoustic Stirling engine”, Nature 1999, 399, 335–338.

[19] T. Biwa, Y. Tashiro, M. Ishigaki, Y. Ueda, T. Yazaki, “Measurements of acoustic streaming in a looped-tube thermoacoustic engine with a jet pump”. J. Appl. Phys. 2007, 101, 064914.

[20] Yazaki, T.; Biwa, T.; Tominaga, A. A piston-less Stirling cooler. Appl. Phys. Lett. 2002, 80, 157–159.

[21] A. Tominaga, Thermodynamic aspects of thermoacoustic theory. Cryogenic 1995, 35, 427–44.